BUTTERWORTH HEINEMANN

Polymer Vol. 36 No. 21, pp. 4023–4030, 1995

0032-3861/95/$10.00 + 0.00

Amorphous orientation of poly(ethylene terephthalate) by X-ray diffraction in combination with Fourier transform infra-red spectroscopy

A. Ajji*, K. C. Cole and M. M. Dumoulin
Industrial Materials Institute, National Research Council Canada, 75 de Mortagne, Boucherville, Québec J4B 6Y4, Canada

and J. Brisson
CERSIM, Département de chimie, Université Laval Québec, Québec G1K 7P4, Canada
(Received 20 February 1995)

Drawing of poly(ethylene terephthalate) (PET) films was performed from the amorphous state using different drawing rates at a temperature of 80°C. The crystallinity of the films was determined by thermal analysis and orientation of the different phases by specular reflection Fourier transform infra-red (*FT*i.r.) spectroscopy and wide-angle X-ray diffraction. The *FT*i.r. spectroscopic and X-ray results showed a significant orientation of the different molecular species (*trans*- and *gauche*-conformers and crystalline phase), particularly for draw ratios (λ) greater than 3. Determination of the amorphous orientation from X-ray diffraction of the amorphous phase of PET is shown to be possible. A combination of the *FT*i.r. results with those obtained for the X-ray orientation of the crystalline phase allowed an independent determination of the amorphous orientation. A good agreement was observed with the corrected X-ray amorphous orientation results for draw ratios greater than 3. Below this draw ratio, low orientation and crystallinity, combined with the inherent limitation of the X-ray technique and crystal imperfections, induced large discrepancies between the two results. It is also shown that the *trans*-conformer orientation increases steadily with draw ratio from the onset of draw and saturates rapidly, whereas that of the *gauche*-conformer is negligible for all draw ratios.

(Keywords: poly(ethylene terephthalate); *FT*i.r. spectroscopy; X-ray diffraction)

INTRODUCTION

The properties of polymeric materials can be enhanced significantly through orientation processes, either in the solid state, in the rubbery state or from the melt. Substantial efforts have been directed towards the orientation of semicrystalline polymers such as polyolefins, polyesters and polyamides[1–6]. In the case of polyesters, the most studied polymer is poly(ethylene terephthalate) (PET) because of its wide use in fibres, films and bottles. However, many questions still remain unclear about its orientation. In fact, conformational changes, the contribution of the interphase, orientation of the amorphous phase, relaxation, and the development of new characterization methods are of great practical and fundamental interest.

To understand the orientation behaviour of PET, it is necessary to start from the simplest structure, i.e. from the amorphous state, which is possible for this polymer because of its relatively high glass transition temperature (T_g) (around 70°C). It has been reported that orientation of amorphous PET above the glass transition temperature is mainly due to the sliding of chains, denoted as flow drawing[7], and does not induce any birefringence in the films. However, other orientation measurement techniques were not used to confirm these observations. In fact, many morphological modifications, such as conformational changes, strain-induced crystallization, and variation in crystal size and distribution, are involved when orienting PET.

The deformation of amorphous isotropic PET films at temperatures slightly above the glass transition temperature under constant load has been described from a molecular point of view[8]. Deformation was qualitatively related to chain relaxation phenomena occurring before stress-induced crystallization, which was then followed by equilibration of a rubber-like network. The junction points include both trapped entanglements and crystalline units. The structure of this network is characterized by the number of segments between the physical cross-links. This parameter was calculated by comparing the predictions of the rubber elasticity theory (without any Gaussian approximation) with the experimentally observed draw ratios under given conditions of temperature and loads. It was shown that small loads induce soft networks, thus leading to high draw ratios. The

* To whom correspondence should be addressed

predictions of the molecular orientation derived from this treatment were in good agreement with birefringence data obtained on a wide variety of samples.

Other researchers have studied the deformation mechanism of amorphous PET as a function of molecular weight and entanglement density in the form of predrawn films[9]. The deformability was shown to be affected by stress-induced crystals, which might act as network points. The tensile modulus and strength of the drawn films were related to draw ratio and molecular weight. The higher the draw ratio and molecular weight, then the higher were the tensile properties of the drawn samples. The improved draw efficiency with higher molecular weights was explained by the suppression of disentanglement and a relaxation of the oriented amorphous molecules during deformation; both are significant in the development of structural anisotropy and continuity along the draw direction.

In all of these cases, the contributions of the different phases as measured by several different techniques were not determined. Determination of the molecular orientation is of critical importance in understanding the properties and structure of oriented materials. Many techniques such as infrared (i.r.) spectroscopy, optical birefringence and X-ray diffraction[1-6] have been developed for the characterization of orientation in polymers.

Fourier transform infra-red spectroscopy coupled with photoacoustic detection (PA-*FT*i.r.) has been shown to be a powerful technique to investigate quantitative structural changes in solid materials[10]. For PET, the results indicated that the structural characteristics of the thermally treated samples are related to the fabrication process. Two different strata in the plates were distinguished, namely a skin layer and the core. The correlation between the apparent degree of crystallinity of the surface, obtained by differential scanning calorimetry (d.s.c.), and the percentage of *trans*-conformer, obtained by PA-*FT*i.r., allowed the latter parameter to be separated into its crystalline and amorphous *trans*-conformer components and also its evolution with the annealing process to be followed. The amorphous *trans*-conformer vanishes at the primary isomerization (100°C), while the crystalline *trans*-conformation shows an approximately linear increase at the expense of the *gauche*-conformation.

Reflection techniques have also been used to characterize the orientation. For PET, polarized internal reflectance spectroscopy has been used to evaluate molecular orientation and crystallinity at the surface of films[11]. Measurements were made on samples stretched in both uniaxial and biaxial modes. All bands of interest were normalized with respect to a reference band near 1410 cm^{-1}, the latter resulting from phenylene ring vibrations. Normalization was performed in order to overcome problems with sample contact and effective thickness. Results obtained by using the bands representing *trans*- and *gauche*-rotational conformers, which are present, respectively, at 1340 cm^{-1} and 1370 cm^{-1}, have been correlated with density and birefringence data. The polarized internal reflectance spectroscopy technique was well suited for investigations of polymer orientation and crystallinity since it avoids limitations related to sample thickness and clarity imposed by polarized transmission i.r. spectroscopy. Parameters such as orientation function, attenuation indices, dichroic ratios and structural factors have been determined from data collected in each of the three spatial directions. Results were found to be in agreement with corresponding density, birefringence, and refractive index data.

However, this technique has some limitations, e.g. the quality of the sample-prism contact and the difficulty in making on-line measurements. A technique based on specular reflection can help to overcome these limitations and yield very useful information on the orientation and structure of oriented PET[12,13]. In particular, it was shown that a quantitative treatment of the specular reflection spectra obtained for uniaxially drawn PET films is possible. Corrections for surface inhomogeneities and an overall orientation function based on *trans*-conformers were calculated. The results have been correlated with mechanical modulus and crystallinity values[13].

A question that is becoming more and more important is the nature of the amorphous phase and its orientation. In a recent paper[14], the behaviour of drawn semicrystalline PET films was investigated by d.s.c., X-ray diffraction and birefringence measurements. The comparison of the different results confirms the coexistence of two structures within the amorphous part of the material: a completely disordered amorphous phase and a mesomorphic amorphous one[14]. Moreover, for the highest draw ratio, the calorimetric results showed that the effect of drawing on the strain-induced crystalline structure is a better orientation of this structure when compared to that obtained through nucleation and growth of new oriented crystallites.

Fluorescence may yield specific information on the amorphous and crystalline phases of PET. In fact, its applicability for obtaining information on the structure of PET has been shown[15]. PET contains two chromophores, namely a monomer (phenyl ring of the monomer unit) and an excimer (excited chromophore dimer). The monomer fluoresces mainly in the crystalline phase, whereas the excimer fluoresces in the amorphous phase. The relationship between the monomer-to-excimer fluorescence intensity ratio and the orientational deformation of PET films was established for structures obtained by isothermal uniaxial orientation. The observed changes in fluorescence intensity ratio were assumed to result from changes in the physical properties (e.g. degree of orientation and crystallinity) of structures that were obtained during the drawing process. However, no other technique was used to confirm these observations.

X-ray diffraction, on the other hand, is a well established technique for the determination of the crystalline phase orientation. The amorphous halo evolves with the degree of crystallinity. Quantitative evaluation of the amorphous phase orientation has been attempted by many researchers[16-21]. However, due to the difficulty of separating the contributions from orientation of the chain and that of the elementary structural unit, it is difficult to determine an absolute value for the orientation function. To overcome this problem, some empirical approaches were developed to relate the observed and true amorphous orientation functions[18-21].

In this present study, we will investigate the orientational behaviour and structure evolution (amorphous,

crystalline and conformers) of PET films. Amorphous PET films were drawn to different draw ratios and the crystallinity was determined by differential scanning calorimetry and orientation by *FT*i.r. spectroscopic and X-ray methods. The orientation of the amorphous phase was determined by the combination of the two techniques and compared to that observed by X-ray studies. Correlation between the orientation value obtained through X-ray and *FT*i.r. measurements was also performed.

EXPERIMENTAL

The material used in this study was an extrusion grade PET without any nucleating agent (Selar PT 7086 from Du Pont) having an intrinsic viscosity (*IV*) of 1. Its molecular characteristics as determined by gel permeation chromatography were $M_n = 28\,800$ and $M_w = 54\,600$. The material was first dried at 90°C for 24 h under vacuum, and sheets were then formed at 280°C by compression moulding in a laboratory press. Amorphous and crystalline sheets were prepared by changing the cooling history (rapid quenching or slow cooling). Thin rectangular films (thickness of 0.1 to 0.6 mm, 1 cm in width and 6 cm in length) were cut from the sheets for orientation and mechanical testing.

Drawing of the films was performed at 80°C in an Instron tensile tester equipped with an environmental chamber. The drawing rate was 2 cm min^{-1}. The draw ratios ranged from 1.2 to 5. The crystallinity of the films before and after orientation was determined from d.s.c. measurements. The crystallization exotherm was subtracted from the melting endotherm to determine the amount of crystallinity initially present in the samples. The enthalpy of melting of completely crystalline PET was taken as 140 kJ kg^{-1} (ref. 22).

Infra-red dichroism measurements were made on a Nicolet 170SX FT-i.r. spectrometer, at a resolution of 4 cm^{-1}, in the reflection mode, by using a versatile reflection accessory with retromirror attachment (Harrick Scientific Corp.). Each spectrum resulted from an accumulation of 128 scans. The angle of incidence used was 20° and a front surface aluminium mirror was used as reference. The samples were attached to the supporting ring supplied with the reflection accessory. Drawn samples were mounted with the draw direction horizontal, i.e. parallel to the plane of incidence. The beam was polarized by means of a quadruple diamond polarizer with silicon plates (Harrick Scientific Corp.). Spectra were measured at two orthogonal polarizations (parallel and perpendicular to the draw direction) without changing the sample position. The Kramers–Kronig transformation was performed with the commercial software, Spectra Calc™ (from Galactic Industries Corporation), using their Maclaurin series algorithm to perform the integration. The details of the calculations of the dichroic ratio and band assignments are published elsewhere[12,13].

X-ray diffraction data were obtained by the use of a Rigaku RU200B rotating anode generator, functioning at 55 kV and 120 mA, using Ni-filtered CuKα radiation. Scattered X-rays were measured by using a scintillation counter. Scans were taken along the equator and meridian in the $\theta-2\theta$ geometry, with the draw direction of the samples placed vertically. For determination of the orientation of the crystalline phase, scans were performed by fixing the 2θ angle at 42.7° and rotating the sample over 180°. For the amorphous phase, the orientation scan was performed at a 2θ position of 12.5°. For these orientation scans, $\chi = 0°$ was defined as the equator position and $\chi = 90°$ as the meridian.

Orientation factors $\langle P_n(\cos\chi)\rangle_{obs}$ (abbreviated as P_n^{obs}) were calculated by using the following equation:

$$\langle P_n(\cos\chi)\rangle^{obs} = \frac{\int I(\chi)P_n(\cos(\chi))\sin(\chi)\,d\chi}{I(\chi)\sin(\chi)\,d\chi} \quad (1)$$

The background level was estimated by linear interpolation using intensities observed before and after the peak in the $\theta-2\theta$ scans and was subtracted prior to estimation of P_n^{obs}. For the amorphous phase orientation measurements, because of the high noise level in the spectra, a Savitsky–Golay smoothing procedure was performed before the orientation calculation.

Since the maximum intensity was not centred at the meridian or 90°, but at 85° for the 0 2 4 reflection and at 0° for the amorphous phase halo, the P_n^{obs} values were corrected using the relationship proposed by Lovell and Mitchell[23], as follows:

$$\langle P_n^{app}\cos\chi\rangle_m = \frac{(-1)^n 2^{2n}(n!)^2 P_n(\cos\chi)^{obs}}{(2n)!} \quad (2)$$

In the case of the crystal-phase peak at $2\theta = 42.7°$ (before calculation) the contribution of a small peak centred at $\chi = 55°$ was removed by spectral decomposition by adjusting the peaks with a Pearson VII peak shape through a least-squares-fitting algorithm.

RESULTS AND DISCUSSION

The crystallinity of PET depends upon many parameters[24,25]. *Figure 1* shows the crystallinity results for initially amorphous samples drawn at a rate of 2 cm min^{-1}. Up to draw ratios of 2–2.5, the stress-induced crystallinity is negligible. As mentioned above, drawing the films induces conformation changes first, then aligns chain segments before crystallization occurs. In fact, the conformation of PET segments in the amorphous state is essentially *gauche* while crystalline PET is constituted solely of *trans*-conformers. Deformation of amorphous PET results in the alignment of the

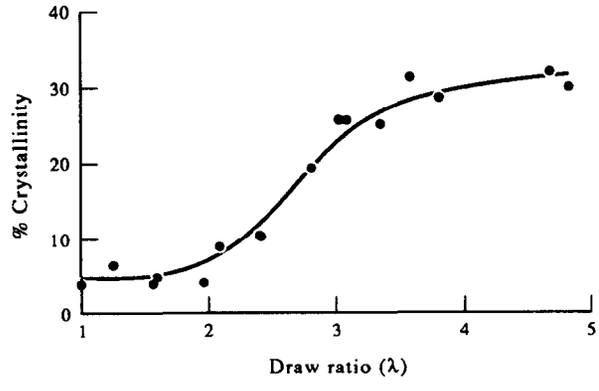

Figure 1 Crystallinity as a function of draw ratio for the amorphous PET films drawn at a rate of 2 cm min^{-1}

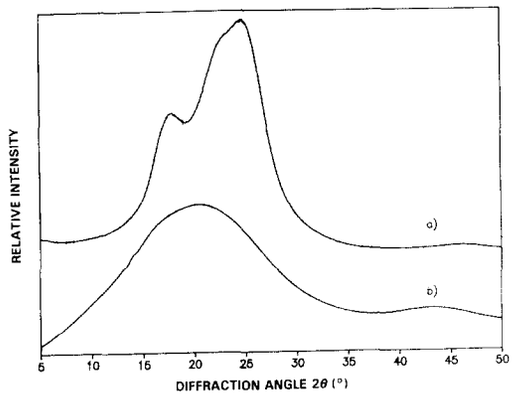

Figure 2 X-ray diffraction equatorial scans of PET samples: (a) crystalline sample ($\lambda = 4.84$); (b) amorphous sample ($\lambda = 1$)

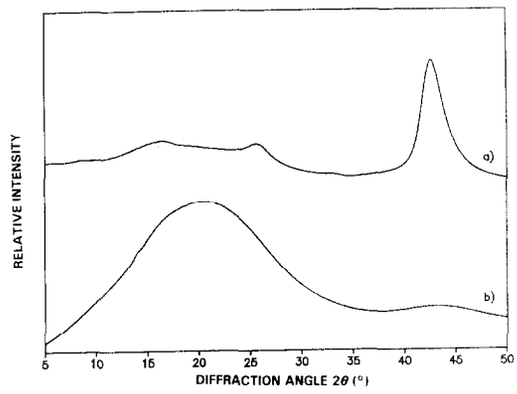

Figure 3 X-ray diffraction meridional scans of PET samples: (a) crystalline sample ($\lambda = 4.84$); (b) amorphous sample ($\lambda = 1$)

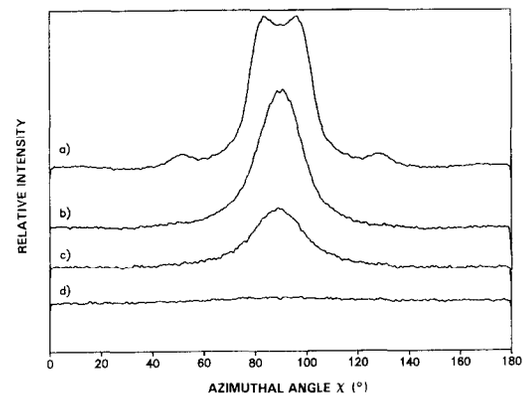

Figure 4 Orientation scans of the (0 2 4) diffraction plane for different values of λ: (a) 4.7; (b) 3.59; (c) 2.9; (d) 2.34

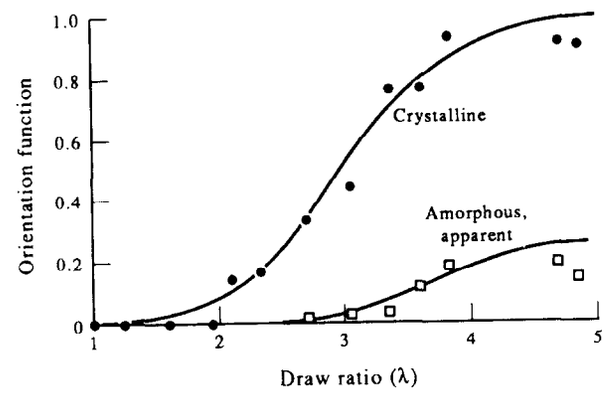

Figure 5 Orientation function as a function of draw ratio for the crystalline and amorphous phases of PET, obtained by X-ray diffraction

trans-conformers in the draw direction and conversion of the *gauche*-conformers into *trans*-conformers. At a certain degree of local order, the aligned chains start to form crystals.

Orientation of the crystalline phase by X-ray diffraction

For PET, the most intense diffraction peaks lie on the equator, in the 18 to 26° region, corresponding to *d*-spacing of 3.4 to 4.9 Å. These were not used for orientation assessment because of the superimposition of the amorphous phase scattering centred at 20°, as can be seen from the equatorial scans of an amorphous and an oriented crystalline sample shown in *Figure 2*. Instead, a less intense diffraction peak was used. It lies at $2\theta = 42.7°$, which corresponds to a *d*-spacing of 2.11 Å, appearing at a χ angle of $\sim 85°$, and showing a medium intensity. As can be seen in *Figure 3*, it is not superimposed with any intense scattering from the amorphous phase. Its assignment is not clear: it has been attributed to the (0 2 4) plane[26], but is often referred to as the (-1 0 5) plane. According to the lattice dimensions proposed by Daubeny *et al.*[26], both would be virtually indistinguishable, the (0 2 4) being at $2\theta = 42.7°$ and a χ of 82.5°, whereas the (-1 0 5) should appear at the same 2θ angle but at a slightly different χ angle of 85.2°. In this work, the assignment of Daubeny *et al.*[26] was used, but the χ angle used was that measured on the most oriented sample. Therefore, the assignment does not have any influence on the orientation parameter determination.

The orientation scans of this diffraction plane are reported in *Figure 4*. It can clearly be seen that, upon increasing λ, the intensity which was distributed evenly along the χ angle starts to centre around the meridian. At high orientation, the peak converges towards the χ position of 85°. In the spectra of the more oriented film, a shoulder can clearly be identified, appearing at a χ angle of $\sim 55°$. This shoulder is attributed to the 2 2 1 reflection, which is reported as having a medium–weak intensity centred at $2\theta = 43.4°$ and $\chi = 50°$. The contribution of this reflection was removed before calculating the orientation factor. The resulting values of the second moment of the orientation function, P_2, calculated using equation (1), are shown in *Figure 5* as a function of draw ratio. No crystalline orientation was observed below a draw ratio of 2 due to the negligible crystallinity present (*Figure 1*), and a saturation is observed for draw ratios above 4.

Orientation of the amorphous phase by X-ray diffraction

X-ray determination of the orientation of the non-crystalline phase is far from being straightforward. The first difficulty arises from choosing a region where no diffraction peaks of the crystalline phase appear. In this particular case, the 12.5° 2θ position was chosen. Although the scattering intensity of the non-crystalline phase is not at its maximum in this region, as can be seen from both *Figures 2* and *3*, it is free from diffraction peaks arising from crystalline domains. On the other

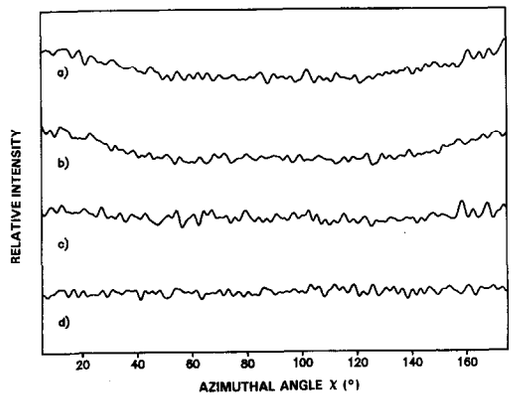

Figure 6 Orientation scans of the amorphous halo ($2\theta = 12.5°$) for different values of λ: (a) 4.7; (b) 3.59; (c) 2.9; (d) 2.34

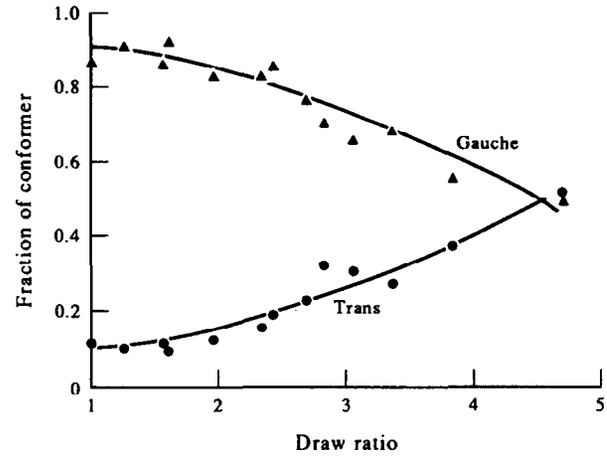

Figure 7 Fraction of *trans*- and *gauche*-conformers of PET as a function of draw ratio

hand, the position where maximum scattering occurs, at around 20°, also coincides with the position where the most intense peaks of the diffraction spectra of the crystal phase occur.

Representative examples of the experimental orientation scans which were used to determine P_2^{obs} appear in *Figure 6*, and the actual values obtained for this orientation factor, using equation (1), are plotted in *Figure 5*. The high level of noise observed in these spectra is directly related to the weak intensity of the amorphous halo at the 2θ position chosen for the experiment. Variations in orientation are nevertheless very apparent. At low orientation, the intensity follows a straight line, with no evident variation with the χ angle. No noticeable orientation can be measured, as reflected by the P_2^{obs} value represented in *Figure 5*. However, at a λ value of around 3, a slight curvature appears in the data, indicating the onset of a very weak orientation. At higher draw ratios, a readily observable orientation can be noted. The amorphous phase orientation seems to follow that of the crystalline phase, although with a much lower value.

The difficulty is, however, not limited to choosing an adequate position: the P_2^{obs} calculated from the experimental data stems in fact from the combination of chain orientation and of the scattering of the elementary unit (e.u.), as follows:

$$\langle P_n(\cos\chi)\rangle^{app} = \langle P_n(\cos\chi)\rangle^{e.u.}\langle P_n(\cos\chi)\rangle \qquad (3)$$

In the case of the crystal phase, the peaks are very narrow, and the elementary unit contribution can be approximated as being equal to unity. However, in the amorphous phase, this approximation is not valid, and this factor has to be estimated before one can have access to orientation factors of the amorphous phase. An empirical method using simplifying assumptions has been proposed as a way to estimate this correction factor. It is based on the determination of an intrinsic azimuthal half-width, from which a correction factor can be determined following the calculations of Pick *et al.*[19]. This intrinsic azimuthal half-width can be determined by plotting the half-width δ of the azimuthal profile, which is obtained by using the following equation[19–21]:

$$\delta = \frac{\int_0^{\pi/2} [I(\chi) - I(0)]\,d\chi}{[I(\pi/2) - I(0)]} \qquad (4)$$

as a function of the observed orientation function, and extrapolating the value of δ for an orientation function of 1. Assuming the validity of the intensity profile proposed by Windle[18] ($I_0(\chi) = 1/(1 + (\chi/\delta)^4)$), it is possible to calculate a correction factor K. The results of these calculations for our data yielded an intrinsic azimuthal half-width of 28°, corresponding to a correction factor of $K = 1.66$[18,19]. The true orientation function P_2 of the amorphous phase from the X-ray measurements will be:

$$P_2 = KP_2^{app} \qquad (5)$$

Application of this correction factor to the data yields a value of P_2 which should correspond reasonably well to the true orientation function of the amorphous phase. These orientation functions will be used to evaluate the validity of this calculation in comparison with the *FT*i.r. spectroscopic results in the following section. Once this factor is validated, X-ray diffraction can be used for the estimation of the amorphous phase orientation.

Determination of orientation by FT*i.r. spectroscopy*

In order to obtain a better idea of the orientation of the drawn films and to compare this with the X-ray results, infra-red dichroic ratio measurements by front surface specular reflection infra-red spectroscopy[12,13] were performed on these films. The questions arising about the correlation of the surface and bulk orientations and structure have already been addressed[12,13,27–29]. In fact, the relative amounts of surface crystallinity and amorphous structure and their respective surface orientations were examined for PET (at depths of 0.5 and 5 mm) by using the attenuated total reflection (ATR) technique[29]. The surface orientation was determined using the i.r. bands at 1340, 1370 and 1410 cm^{-1} (ref. 27). The results indicated a higher degree of extended *trans*-segments and a higher degree of extended chain orientation near the surface in the draw direction relative to the bulk of the film. An increased crystallinity at the surface was also observed.

Figures 7 and *8* show, respectively, the conformers' fraction and orientation function obtained by the specular reflection technique as a function of draw ratio λ for the *gauche*- and *trans*-conformers. The details

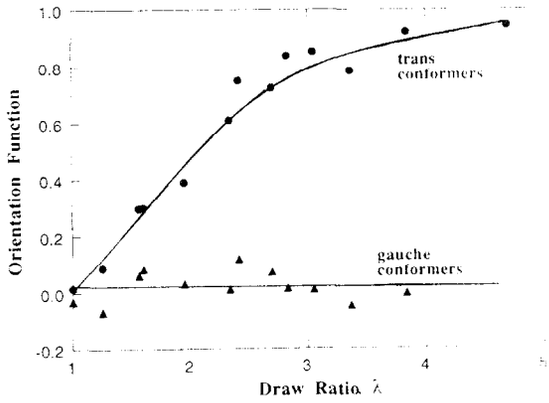

Figure 8 Orientation function of the *trans*- and *gauche*-conformers of PET as a function of draw ratio, as determined by *FT*i.r. spectroscopy

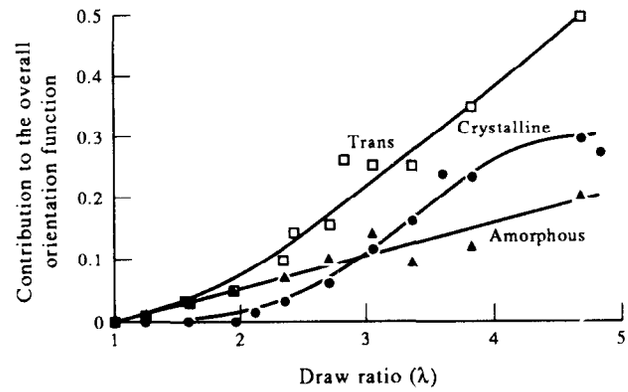

Figure 9 Orientation contributions of the *trans*-, crystalline and amorphous phases of PET to the overall orientation function as a function of draw ratio

of the measurements and calculations are presented elsewhere[12,13]. The results clearly indicate an alignment of the chains' *trans*-segments along the direction of draw for all draw ratios. For the *gauche*-conformers, negligible orientation is observed for all draw ratios. Since this conformation is present only in the amorphous phase, this indicates that the amorphous phase is not significantly oriented. It is also observed that the *trans*-conformer orientation saturates (very close to 1) at λ values of around 4. Considering the structure of the drawn films (*Figure 7*), a gradual conversion of the *gauche*- to *trans*-conformers is observed. It is to be noted that the *trans*-content is in all cases higher than the crystalline fraction (*Figure 1*), indicating that a fraction of the *trans*-conformers is present in the amorphous phase.

In the cases where significant crystallinity was obtained, orientation of the crystalline phase was determined by wide-angle X-ray diffraction as presented in the previous section. The results obtained for the crystalline orientation function were presented in *Figure 5*. There is no crystalline orientation for λ values below 2. In fact, the crystalline-phase content in this region is negligible according to *Figure 1*. However, according to *Figure 8*, orientation of the *trans*-conformers increases from the beginning of drawing. It is to be noted also that the crystalline orientation is lower than that of the *trans*-conformers up to draw ratios of ~ 3.5. At first sight, knowing that the crystalline phase is constituted only of *trans*-conformers, this result may seem surprising. However, since the crystalline-phase content starts to be significant only for λ values above 2, the absence of amorphous orientation below a λ of 2 is normal. The development of crystallites during deformation at low rates is known to induce the presence of a certain number of imperfections[30]. In fact, when the *trans*-conformers' orientation is measured by *FT*i.r. spectroscopy it reflects the order of specific bands on the molecular level, whereas the crystalline orientation describes that of larger assemblies. With the observations mentioned above concerning the crystalline arrangements and perfection obtained upon stress-induced crystallization at low deformation rates, this result seems reasonable.

In fact, Gupta *et al.*[30] studied the degree of crystal perfection in semicrystalline PET fibres and films produced under different conditions with the help of X-ray diffraction. Fibres and films which were produced by low-speed melt extrusion, followed by drawing in water at low strain rates in a low-temperature environment, had the lowest X-ray crystallinity and the most imperfect crystals. Further evidence of greater crystalline imperfection in these samples was provided by their X-ray intensity plots and melting endotherms. The low X-ray crystallinity and high defect density shown by these samples have been attributed to the slow drawing at relatively low temperatures. Such conditions do not provide the necessary environment for crystallization. The presence of very small nuclei may also be a cause of sample imperfections. These small nuclei are crystalline remnants that are retained at low production speeds, with crystallization occurring around those defects.

Estimation of amorphous orientation through combination of the FT*i.r. spectroscopic and X-ray diffraction results*

The overall orientation can be written as follows:

$$f_{\text{overall}} = f_{trans}X_{trans} + f_{gauche}X_{gauche} \tag{6}$$

or

$$f_{\text{overall}} = f_{\text{cryst}}X_{\text{cryst}} + f_{\text{amor}}X_{\text{amor}} \tag{7}$$

where f designates the second moment of the orientation function and X the volume fraction of the phase being considered. The form contribution arising from the crystalline–amorphous interface is neglected. The contribution of the amorphous phase to the overall orientation function can be obtained by using the different results presented previously. The overall orientation (from equation (6)) is presented in *Figure 9*, as well as the crystalline contribution (i.e. $f_{\text{cryst}}X_{\text{cryst}}$) and the calculated amorphous contribution (i.e. $f_{\text{amor}}X_{\text{amor}}$). At the beginning of the orientation process, the X-ray results give systematically lower orientation values than the *FT*i.r. spectroscopic measurements. In fact, the amorphous phase is composed primarily of *gauche*-conformers whose orientation is negligible. With the increase in deformation, the *trans*-content becomes larger both in the amorphous and the crystalline phases, and the *FT*i.r. orientation function of the amorphous phase becomes significant.

The amorphous orientation function was determined from the calculated amorphous contribution,

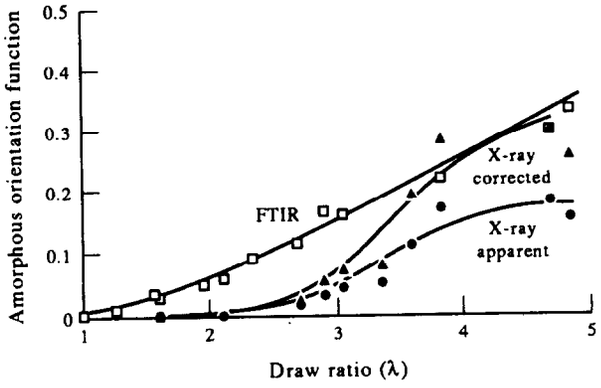

Figure 10 Orientation function of the amorphous phase of PET, determined by different methods, as a function of draw ratio

i.e. $f_{amor}X_{amor}$, by dividing by the amorphous content. This result, together with the observed and corrected X-ray amorphous orientation functions, is presented in *Figure 10*. First, it can be clearly seen that the observed uncorrected X-ray amorphous orientation is lower than that determined from a combination of the *FT*i.r. and X-ray crystalline phase results, which is in agreement with the literature data[19–21]. Secondly, the corrected X-ray amorphous orientation is in good agreement with that determined from a combination of the *FT*i.r. and X-ray methods for high draw ratios (greater than 3). However, one has to keep in mind the relatively low degree of crystallinity and crystal perfection for draw ratios below 3, and the experimental errors arising from the determination of both the crystalline and amorphous orientations. An additional cause of error stems from the modes of measurement: *FT*i.r. spectroscopy is representative of the polymer surface, whereas X-ray scattering is representative of the whole sample thickness.

Up to a draw ratio of 3, no significant orientation was detected by the X-ray measurements. This difference with respect to the *FT*i.r. method is believed to be intrinsic to the phenomena involved in X-ray scattering. It is well established that the peaks which are observed between 10 and 30° stem from the interference of X-rays scattered by adjacent chains which lie at relatively constant distances from one another, as a result of stacking constraints. These are due to the tendency of matter, even in the amorphous phase, to minimize free volume and maximize attractive interchain interactions (van der Waals, electrostatic), while minimizing repulsive interactions. During the first stages of drawing, if a chain orients while its neighbours have not yet begun to do so, the interference between the segments of these chains will lead to an isotropic scattering pattern along the azimuthal direction, and will therefore not contain the information on orientation. Furthermore, as demonstrated by the *FT*i.r. measurements, in the first stages of orientation, conformational changes dominate over true chain orientation. These will not be detected by X-ray scattering and will therefore not contribute to the measured orientation function. When the draw ratio increases further (above a value of 3), the number of oriented chain segments increases, and after a while, small domains of adjacent oriented chain segments begin to appear, leading this time to an anisotropy in the scattered X-rays which undergo interference to yield the characteristic scattering pattern. This pattern is then anisotropic, and the orientation can be calculated as described earlier. The differences between the results from the two techniques will then vanish and remaining fluctuations will stem mainly from experimental errors, as described above.

CONCLUSIONS

Determination of the amorphous orientation of PET from X-ray scattering data has been shown to be possible. The correction factor for the observed X-ray amorphous orientation was estimated, by using the scattered peak width, to be 1.66. A combination of *FT*i.r. spectroscopic and X-ray orientation results allowed an independent determination of the amorphous orientation. A good agreement was observed with corrected X-ray amorphous orientation results for draw ratios above a value of 3. Below this draw ratio, the intrinsic limitations of the technique, combined with cumulative experimental errors and crystal imperfection, induced large discrepancies between the X-ray corrected amorphous orientation and that obtained from a combination of *FT*i.r. and X-ray results. From the *FT*i.r. orientation results, it has also been shown that the *trans*-conformer orientation increases steadily with draw ratio from the onset of draw and saturates rapidly, whereas that of the *gauche*-conformer is negligible for all draw ratios.

REFERENCES

1 Samuels, R. J. 'Structured Polymer Properties', Wiley, New York, 1974
2 Zachariades, A. E. and Porter, R. S. 'The Strength and Stiffness of Polymers', Marcel Dekker, New York, 1983
3 Zachariades, A. E. and Porter, R.S. 'High Modulus Polymers', Marcel Dekker, New York, 1988
4 Ward, I. M. 'Structure and Properties of Oriented Polymers', Applied Science, London, 1975
5 New Advances in Oriented Polymers, Proceedings of SPE RETEC, Atlantic City, NJ, September 1987
6 Ward, I. M. *Adv. Polym. Sci.* 1985, **70**, 1
7 Radhakrishnan, J. and Gupta, V. B. *J. Macromol. Sci. Phys.* 1993, **32**, 243
8 Lorentz, G. and Tassin, J. F. *Polymer* 1994, **35**, 3200
9 Huang, B., Ito, M. and Kanamoto, T. *Polymer* 1994, **35**, 1210
10 Quintilla, L., Rodriguez-Cabello, J. C., Jawhari, T. and Pastor, J. M. *Polymer* 1993, **34**, 3787
11 Lofgren, E. A. and Jabarin, S. A. *J. Appl. Polym. Sci.* 1994, **51**, 1251
12 Cole, K. C., Guèvremont, J., Ajji, A. and Dumoulin, M. M. *Appl. Spectrosc.* 1994, **48**, 1513
13 Guèvremont, J., Ajji, A., Cole, K. C. and Dumoulin, M. M. *Polymer* in press
14 Dargent, E., Grenet, J. and Auvray, X. *J. Therm. Anal.* 1994, **41**, 1409
15 Kalechits, I. I., Kuzmin, M. G. and Banatskaya, M. I. *Vysokomol. Soedin. Ser. A/B* 1993, **35**, B1701
16 Biangardi, H. J. *J. Polym. Sci., Polym. Phys. Edn* 1980, **18**, 903
17 Biangardi, H. J. *Makromol. Chem.* 1982, **183**, 1785
18 Windle, A. H. in 'Development in Oriented Polymers', Vol. 1 (Ed. I. M. Ward), Applied Science, London, 1982, p. 1
19 Pick, M., Lovell, R. and Windle, A. H. *Polymer* 1980, **21**, 1017
20 Vancso, G., Snétivy, D. and Tomka, I. *J. Appl. Polym. Sci.* 1991, **42**, 1351
21 van Aerle, N. A. J. M. and Tol, A. J. W. *Macromolecules* 1994, **27**, 6520
22 Wunderlich, B. *Polym. Eng. Sci.* 1978, **18**, 431
23 Lovell, R. and Mitchell, G. R. *Acta Crystallogr. Sect. A* 1981, **37**, 135
24 Jabarin, S. A. *Polym. Eng. Sci.* 1992, **32**, 1341

25 Kaito, A., Nakayama, K. and Kanetsuna, H. *J. Polym. Sci., Polym. Phys. Edn* 1988, **26**, 1439
26 Daubeny, R. de P., Bunn, C. W. and Brown, C. J. *Proc. R. Soc. London A* 1954, **226**, 531
27 Walls, D. J. *Appl. Spectrosc.* 1991, **45**, 1193
28 Mirabella, F. M. *J. Polym. Sci., Polym. Phys. Edn* 1984, **22**, 1293
29 Walls, D. J. and Coburn, J. C. *J. Polym. Sci., Polym. Phys. Edn* 1992, **30**, 887
30 Gupta, V. B., Jain, A. K., Radhakrishnan, J. and Chidambareswaran, P. K. *J. Macromol. Sci. Phys.* 1994, **33**, 185